Talanta
January 2021, Volume 221 Pages 121589 (7p.)
https://doi.org/10.1016/j.talanta.2020.121589
https://archimer.ifremer.fr/doc/00686/79819/

Determination of rare earth elements in gadolinium-based contrast agents by ICP-MS

Ben Salem Douraied [1, *], Barrat Jean-Alix [2]

[1] LaTIM (INSERM UMR 1101) Université de Bretagne Occidentale. 22, Avenue C. Desmoulins, 29238, Brest Cedex 3, France
[2] Univ Brest, CNRS, UMR 6539 (Laboratoire des Sciences de L'Environnement Marin), LIA BeBEST, Institut Universitaire Européen de La Mer (IUEM), Place Nicolas Copernic, 29280, Plouzané, France

* Corresponding author : Douraied Ben Salem, email address : douraied.bensalem@chu-brest.fr

Abstract :

A simple ICP-MS procedure for the determination of trace element concentrations in GBCAs is described here. Abundances of most of the REEs, Y, Ba and Pb concentrations were determined. We confirm that GBCAs contain traces of non-Gd REEs, Y, Ba and Pb. REE patterns of the five GBCAs actually administered in France have been obtained. They display specific shapes that make it possible to identify the different Gd oxides oxides used by pharmaceutical laboratories to produce them. Our method enables us to quickly evaluate the quantities of impurities in these products and, if necessary, to follow the evolution of their quality in the future. The presence of small but not negligible quantities of Y and REEs other than Gd cannot be ignored in these products, and their behaviour in the human body must be considered. The concentrations measured for Pb and Ba, on the other hand, are much lower and do not pose any particular problems.

Graphical abstract

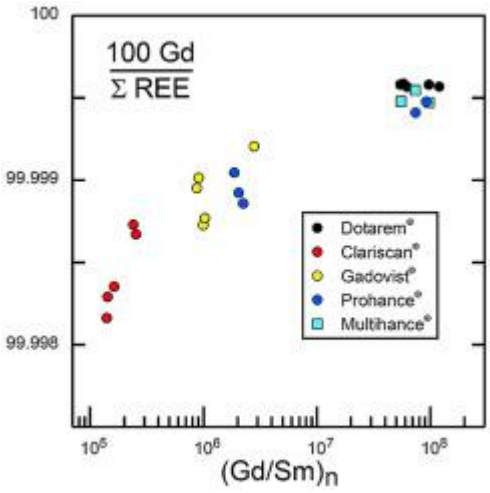

Highlights

► A method was developed for the analysis of trace elements in GBCAs by ICP-MS. ► Ba, Pb, Y and most of the non-Gd REEs are easily and accurately determined. ► Low amounts of Y and non-Gd REEs are present in all the GBCAs currently in use in EU. ► The presence of Y and non-Gd REEs in GBCAs may be a matter of concern.

Keywords : Gadolinium based contrast agent (GBCA), Trace elements, Rare earth elements, ICP-MS, Magnetic resonance imaging (MRI)

1. Introduction

Since their introduction in the late-1980s, linear or macrocyclic Gd-based contrast agents (GBCAs) have significantly improved the diagnostic accuracy of magnetic resonance images (MRI), thereby facilitating the monitoring of many diseases [e.g., 1-4]. About thirty million patients each year have GBCA injections before a MRI exam [2]. Although in the vast majority of cases, Gd is rapidly eliminated by the body and GBCA injections do not present any significant risk, various adverse effects have been reported. The most serious is nephrogenic systemic fibrosis, a rare and sometimes lethal disease that can occur in patients with renal failure

after exposure to linear GBCAs [5]. In addition, numerous studies have reported cases of accumulation of Gd in skin, bone and even the brain after GBCA injections in patients without renal failure [e.g., 6]. As a result, the use of linear GBCAs has been considerably reduced, and most of them are now banned in the European Union [7]. The consequences of such accumulations are not well known and are being studied by many teams [e.g., 8]. Another source of problems could be trace elements in the injected solutions. This possibility should at least be discussed or mentioned since a recent study has just highlighted small but non-negligible quantities of other rare earth elements (REEs) that accompany Gd [9]. These elements are potentially toxic and could also be the cause of undesirable side effects [10, 11].

The aim of this work is double. First, to develop a simple methodology to determine the concentrations of rare earths other than Gd in GBCAs, and possibly to detect and quantify the contents of other trace elements in these solutions. Secondly, Veiga et al. [9] presented data for REEs contained in a series of GBCAs used in the South American market, but except for two of them, they are not or no longer used in the European Union (EU) [7]. Additional data are thus necessary for the GBCAs currently commercialized.

The determination of REEs in different types of material is routinely carried out by ICP-MS by many geochemistry laboratories. Adaptation of well-established methods is possible. However, GBCA analysis poses specific problems. Generally, when REE contents are low, separation and preconcentration techniques are commonly used to separate them from major elements. Here, this is not possible because Gd is a REE and a major element of the product to be analyzed. It is not possible to remove or separate it without fractionating the abundances of the other REEs present in much smaller quantities. Furthermore, the oxides and hydroxides of Gd are known to produce isobaric interferences when analyzed by ICP-MS and are additional complications in the analytical work. Here, we present a simple procedure for the determination of trace elements in GBCAs, adapted from our routine method that we developed for rock

75 samples [e.g., 12-15]. We present here the results obtained on a sampling of the various GBCAs
76 used today in EU.

77

78 2. Experimental techniques

79 Sample preparation

80 We have selected samples of all the GBCAs allowed in the EU today: 5 samples of
81 Dotarem® (gadoterate meglumine, Guerbet), 5 samples of Clariscan® (gadoterate meglumine,
82 GE Healthcare SAS), 5 samples of Gadovist® (gadobutrol, Bayer AG), 5 samples of ProHance®
83 (gadoteridol, Bracco Imaging), and 3 samples of MultiHance® (gadobenate dimeglumine,
84 Bracco Imaging). All samples are from different lots, except for two samples of Clariscan®
85 (samples D and E), and two of Gadovist® (samples D and E).

86

87 All preparations were conducted in a Class 1000 (ISO 6) clean laboratory. Samples were
88 taken directly from the vials (MultiHance®) or from the syringe outlets. Two aliquots weighing
89 about 75 mg each, were taken per sample, and were accurately weighed into 30 ml screw-top
90 Teflon vials. One of them was precisely spiked with a solution of pure Tm. The spike solution
91 was previously prepared with a Tm mono-elementary solution (custom grade, CGTM1-1,
92 Inorganic Ventures Inc.®), and is routinely used in our laboratory for trace element analyses by
93 ICP-MS [e.g., 12-15]. About 60-70 ng of Tm was added for 75 mg of sample.

94 Deionized water purified with a Milli-Q system (Millipore®) at 18.2 MΩ (referred to
95 hereafter as ultrapure water) was used for material cleaning and acid dilutions. Nitric acid was
96 purified using a sub-boiling system.

Samples were dried at 105°C on a hot plate. The residues were taken up with one drop of conc. HNO_3 in order to oxidize eventual organic traces, dried again and taken up in 10 ml of 0.4 N HNO_3 with traces of HF (6 drops of sub-boiled HF per litre). About 0.3 ml of these solutions were diluted before analysis with 4 ml of 0.4 N HNO_3 with traces of HF. Their dilution factors (solution mass/sample mass) were equivalent to 3800-4000. Based on the Gd content indicated by the manufacturers, their Gd concentrations ranged from 15 to 35 µg/g.

Mass spectrometry

The measurements were performed on a Thermo Scientific ELEMENT XR™ spectrometer located at the "Pôle Spectrométrie Océan", Institut Universitaire Européen de la Mer, Plouzané. Basic operating conditions, and selected masses are summarized in Table 1. Data were acquired with a routine sequence using the software supplied by the manufacturer, and processed as already reported in earlier studies. The reader is referred to previous papers where our routine sequence, calibration and calculations of concentrations with the Tm spike have been extensively described [e.g., 12-15]. Briefly, Ba and REE oxides, and hydroxide formation rates were determined by analysing solutions of ultrapure water, Ba+Ce, Pr+Nd, and Sm+Eu+Tb at the beginning of the analytical session. During the course of the study, these rates remained systematically < 0.1 % for $CeOH^+/Ce^+$. Measured sample data were corrected for the contribution of procedural blank, drift, and interferences assuming constant rates of oxide and hydroxide formation during the session.

The determination of trace element abundances in GBCAs however requires some adaptations to our protocol designed for geological samples. Previous analyses of GBCAs showed that these products are poor in REEs other than Gd [9]. To determine them with sufficient accuracies, it is tempting to use solutions that are not too diluted. However, the Gd

richness of the latter can induce excessive washing times between samples. The dilution factors chosen here (of the order of 3800-4000) are good compromises, and allow the measurement of most of the REEs other than Gd, as well as a couple of other elements, as we will see below. Analyses are nevertheless complicated by the formation of isobaric GdO^+ or $GdOH^+$ interferences, which are too large be corrected by conventional procedures, or perfectly resolved in high resolution mode. Some of these interferences are illustrated in Figure 1. In the case of geological samples, the determination of Tm, Yb and Lu concentrations is possible with the masses 169 (^{169}Tm), 174 (^{174}Yb), and 175 (^{175}Lu). The observed interferences are generally of moderate or of low importance and easily correctible for these samples [e.g., 12, 16]. In the case of GBCAs, extremely large interferences are observed for all these masses. The nice straight lines obtained with the signal measured for a minor Gd isotope and those measured for these masses, and the fact that these lines pass through the origin, indicate that the signals are essentially produced by isobaric interferences of GdO^+ or $GdOH^+$, but also that the concentrations of these three elements in GBCAs are extremely low. High-resolution measurements did not completely remove these interferences. Similarly, significant interferences are measured on masses 177 and 178 which are usually used to quantify the abundances of Hf. The abundances of this element in GBCAs are too low, and require a different protocol (e.g., isotope dilution and chemical separation).

At first glance, the use of a Tm spike could be more complicated for the analysis of GBCAs than for geological samples. Firstly, the formation in the plasma of major isobaric interferences ($^{152}Gd^{17}O^+$ or $^{152}Gd^{16}OH^+$) on mass 169 ($^{169}Tm^+$) must be taken into account. Secondly, the Er and Yb abundances cannot be used to interpolate the Tm abundances in these compounds as we do with rocks [12], because Yb abundances are not determined. These two drawbacks can be directly addressed by using a sufficient quantity of spike, on the one hand, and, on the other hand, by analysing, during the same session, a solution of the same sample

146 without spike. The amount of spike we used per sample is such that the signal produced by the
147 added Tm is more than 10 times greater than the isobaric interferences on mass 169 and the Tm
148 initially contained by the sample. The element abundances in spiked (C_{X1}) and unspiked (C_{X2})
149 solutions were determined in triplicates, and averaged. The trace element abundances in the
150 samples ([X] in µg/g) were calculated using the following equations adapted from Barrat et al.
151 (1996):

152 $$[X] = (M_{Tm} \,.\, C_{X1}) / (M \,.\,. \, C_{Tm1}^*) \qquad (1)$$

153 where M_{Tm} is the amount of Tm (in µg) added in the spiked solution, M the mass of
154 spiked sample (in g), and C_{Tm1}^* the concentration of Tm brought by the spike in the spiked
155 solution. C_{Tm1}^* is estimated using the results obtained with the unspiked solution:

156 $$C_{Tm1}^* = C_{Tm1} - (C_{Tb1} \,.\, C_{Tm2} / C_{Tb2}) \qquad (2)$$

157 C_{Tm1} and C_{Tm2}, the Tm concentrations we calculate in solutions, are always
158 overestimated due to the contribution of Gd isobaric interferences. However, since the rates of
159 oxide and hydroxide production during the ICP-MS session can be considered constant, since
160 spiked and unspiked solutions of the same samples are measured a few minutes apart, and since
161 the signal produced by Tm added to the spiked solution is well above 90 % of the signal
162 produced by the isobaric interferences and the Tm initially present in the sample, the calculation
163 of C_{Tm1}^* is not significantly affected by the interferences. We checked our procedure and
164 equations using solutions of Allende USNM3529, a rock standard displaying a large positive
165 Tm anomaly. Our results are similar to reference and literature values and confirm the validity
166 of our procedure (Table 2).

167
168
169
170

3. Results and discussion

All our GBCA samples display very low abundances of trace elements. With the dilutions we used, the signals obtained for many elements and the instrumental blanks were often similar. Thus we did not either estimate their concentrations, or their detection limits. Among the forty or so elements we measured (Table 1), signals were large enough for Y, Ba, REEs and Pb, and the results for these elements are reported in Table 2.

Barium concentrations are < 102 ng/g and Ba/Eu ratios are always < 10. Therefore, isobaric interferences of Ba oxides or hydroxides on Sm and Eu were low or insignificant, and were very easily corrected. Neodymium, Sm and Eu are also in low quantities, and the isobaric interferences they produced on Tb, Dy, Ho and Er, were also easily corrected. The situation is different for Tm, Yb, Lu and Hf, which are very low and not determinable with our method, because of the major isobaric GdO^+ and $GdOH^+$ interferences as we have shown above.

Since the sixties, geochemists usually normalize the REE abundances to those of a reference, generally a CI chondrite, in order to compare the abundances of materials and to highlight some of their remarkable features [e.g., 17, 18]. Smooth patterns with possible Eu or Ce anomalies are obtained for natural terrestrial materials. Also commonly added to this diagram is Y, which has chemical properties comparable to Ho (same valence and ionic radius). In the case of GBCAs, huge fractionations are predictable because their REEs result from an industrial process. Although their REE patterns may differ from those of natural materials, these diagrams can be very useful for comparing GBCAs with each other.

CI-chondrite normalized REE patterns of GBCAs are plotted in Figure 2. The following observations emerge:

- The REE patterns of GBCAs are extremely unusual, and show huge positive Gd anomalies. Normalised abundances vary over 7 to 9 orders of magnitude depending on the GBCAs.

- The patterns obtained are quite variable. Except for Prohance®, the batches of each GBCA give fairly consistent results. Dotarem® and MultiHance® have similar patterns, which are very different from those obtained for Clariscan® and Gadovist®. ProHance® exhibits two types of patterns. Two batches (B and C) have patterns comparable to those of MultiHance® or Dotarem®, suggesting the use of the same Gd concentrate. The three other batches of ProHance® were produced with a distinct Gd concentrate, whose REE pattern resembles that of Gadovist®. Veiga et al [9] also analysed Dotarem® and Gadovist®. Their results for Gadovist® are very similar to ours. On the other hand, their Dotarem® batches were slightly richer in La, Pr, and Nd than those available to us, suggesting the use of a different Gd concentrates for the production of these GBCAs.

- All the patterns show increasing normalized concentrations from Sm to Gd and decreasing normalized concentrations from Gd to Dy. This property certainly results from industrial processes for Gd purification. The chondrite-normalised ratios $(Gd/Sm)_n$ and $(Gd/Dy)_n$ are very high and vary respectively from $1.4x10^5$ to $1.2x10^8$, and from $7.2x10^5$ to $6.6x10^6$ depending on amounts of non-Gd REEs in the GBCAs (Fig. 3).

- The relative proportions of light REEs (from La to Sm) and of the heaviest REEs measured here (Dy to Er), are variable from one GBCA to another. Marked anomalies are present. For example, Gadovist® patterns systematically show pronounced negative anomalies in Ce, and Clariscan® patterns systematically show positive anomalies in La.

- All GBCAs have negative Y anomalies [$(Y/Ho)_n$=0.03-0.5] except Clariscan® which has positive Y anomalies [$(Y/Ho)_n$=2.7-3.5].

- The Tm, Yb and Lu abundances cannot be determined with our procedure because of the large isobaric interferences which could not be corrected (see above). Usual geochemical or cosmochemical reasoning for compounds resulting from industrial enrichment processes may

of course be questionable. However, the shape of the patterns provides some constraints on the concentration levels in Tm, Yb and Lu which were not determined. Large positive anomalies in Tm, Yb and Lu are unknown in terrestrial rocks [e.g., 14] and consequently in REE ores. It is therefore more than unlikely that such anomalies are present in GBCAs. Thus, chondrite-normalised abundances of these elements cannot be higher than those of Er. Using this constraint, we can estimate upper limits for their abundances. For Dotarem® and MultiHance®, Tm and Lu are necessarily < 0.2 ng/g, and Yb < 1.1 ng/g, for Clariscan®, Tm and Lu < 0.1 ng/g, Yb < 0.5 ng/g, for Gadovist, Tm and Lu < 8.6 ng/g, Yb < 54 ng/g, and for ProHance®, Tm and Lu < 0.5 ng/g, and Yb < 3.1 ng/g. These concentrations are very low and consistent with what could be inferred from examination of the raw data (Fig. 1a). Considerably higher Tm concentrations (> 100 ng/g) were measured by Veiga et al. [9] in all their samples (e.g., ≈ 130 ng/g in Dotarem®, and ≈ 205 ng/g in Gadovist®). These large discrepancies most certainly result from isobaric interferences of $GdOH^+$ on Tm, not taken into account by these authors.

In principle, there are different possible origins for the trace elements contained in syringes and vials of GBCAs. First, they can be derived from the Gd concentrates used to produce these products. A fraction of them could also have been introduced with the reagents used to form chelates, with the excipients, or introduced during the packaging of the solutions. It is reasonable to assume that the REE patterns of reagents, excipients, or any potential pollution in production lines should be similar to those of ordinary geological materials. The levels of non-Gd REEs in GBCAs are very low (much lower than the chondritic concentrations in most of our samples), and therefore very easy to contaminate. Any contamination in the GBCA production and packaging lines would inevitably tend to increase the concentrations of non-Gd REEs, but also to erase all the anomalies shown by the REE patterns. The low abundances of non-Gd REEs in commercial solutions of GBCAs, coupled with their marked anomalies shown by their REE patterns, suggests that undesired REEs were not introduced

during the process. It is indirect evidence of the excellence of the GBCA production and packaging lines. We conclude that the relative proportions of REEs in GBCAs are identical to those of the Gd concentrates used to prepare them. The diversity of the REE patterns of the five GBCAs analysed here also shows that Gd concentrates used by the different laboratories have not all been subject to the same level of purification. The Gd concentrates used to produce the Clariscan® are richer in non-Gd REEs than those used to produce Dotarem® or MultiHance® (Fig. 3a and Table 2). Those used to produce Gadovist® and ProHance® are of intermediate quality. This difference in quality is also marked by higher Y and Pb concentrations in Clariscan® than in the other GBCAs (Fig. 2 and 3b). However, this observation is based only on the analysis of batches produced over a period of a few months, and obviously does not prejudge the quality of the Gd and the reactants used in the past or in the future by pharmaceutical companies.

In agreement with Veiga et al. [9], GBCAs contain measurable amounts of REEs other than Gd. These amounts, although small, are analytically well quantifiable and range on average from 280 ng/g (330 ng/ml) for Dotarem® to 1340 ng/g (1750 ng/ml) for Gadovist®. Veiga et al [9] reported values of the same order of magnitude for Dotarem® and Gadovist® (660 ng/ml and 1650 ng/ml, respectively). The differences are small but the results from the two studies cannot be directly compared. They can be explained by the possible heterogeneities of the GBCAs batches, by the fact that Veiga et al. [9] did not determine Sm and included Y and Sc with the REEs, and finally that their Tm concentrations were most probably overestimated due to interferences that were not taken into account. In addition to the traces of REEs, Y, Ba and Pb are also present. We have estimated the average quantities of these impurities injected into a 70 kg adult individual (Fig. 4) by applying the recommended dosage (0.1 ml/kg for Gadovist® and 0.2 ml/kg for other GBCAs). The behaviour of the non-Gd REEs in the body is certainly dependent on their speciation. Due to the similarities of the chemical properties of REEs, we

can reasonably assume that they were chelated similarly to Gd during the production of GBCAs. The same is probable for Y that could behave like Ho due to its valence and the similarity of its ionic radius. The behaviour in the human body of the non-Gd REE and Y chelates are not well known, and could be less stable than Gd chelates. It cannot be ruled out at this stage that these elements may become fixed in the same tissues as Gd [19], but this hypothesis needs to be confirmed by further work. In the analysed batches, the levels of Ba and Pb are low and should not pose any particular toxicity problems [e.g., 20].

4. Conclusions

Except for the three heaviest REEs (Tm, Yb, Lu) which are in low abundance and whose signals are largely masked by GdO^+ or $GdOH^+$ isobaric interferences, the determination of concentrations of non-Gd REEs and some other trace elements such as Y, Ba and Pb in GBCAs can easily be performed by ICP-MS.

We determined the REEs, Y, Ba and Pb abundances in samples of the five GBCAs currently used in France. Their trace element distributions make it possible to identify the Gd concentrates used for their production. Dotarem® and MultiHance® samples are those that contain the least non-Gd REEs and Y. Their REE+Y patterns suggest that they were made from the same Gd concentrates. Gadovist® and Clariscan® samples were made from separate Gd concentrates, containing significantly more impurities. ProHance® samples were produced with Gd concentrates identical to those used for MultiHance® for some batches, and Gadovist®-like concentrates for other batches. In any case, our results confirm that the GBCA solutions contain measurable amounts of non-Gd REEs and Y. The behaviour of these elements in the human body, including their possible accumulation in certain tissues such as skin, bone and brain, should be considered and studied. The data we publish here, as well as our methodology, can

be used to compare and estimate the levels of impurities in GBCAs that will be produced in the future.

Acknowledgements: We thank Jean-Michel Kauffmann for the editorial handling, the reviewers, Raphaël Tripier, Roger Hewins, and Michel Rafini for constructive comments or corrections. ICP-MS analyses were obtained with the help of Bleuenn Gueguen and Marie-Laure Rouget. This work was supported by the "Laboratoire d'Excellence" LabexMER (ANR-10-LABX-19) and funded by grants from the French Government under the program "Investissements d'Avenir".

CRediT authorship contribution statement

Douraied Ben Salem, Jean-Alix Barrat : Conceptualization, Methodology, Investigation, Validation, Writing.

Declaration of competing interests

Douraied Ben Salem declare that he has conflict of interest with Philips France, Toshiba Medical France, Genzyme, Biogen France, Boston Scientific, Bracco Imaging France, Guerbet France, GE Medical system.

Jean-Alix Barrat declare that he have no known competing financial interests or personal relationships that could have appeared to influence the work reported in this paper.

References

[1] V.M. Runge, M.L. Wood, D. Kaufman, A.C. Price, Gd DTPA. Future applications with advanced imaging techniques. Radiographics 8 (1988), 161-179.

[2] J. Lohrke, T. Frenzel, J. Endrikat *et al.*, 25 Years of Contrast-Enhanced MRI: Developments, Current Challenges and Future Perspectives. Adv Ther.33(2016), 1-28.

[3] F. Lersy, G. Boulouis, O. Clément *et al.*, Consensus Guidelines of the French Society of Neuroradiology (SFNR) on the use of Gadolinium-Based Contrast agents (GBCAs) and related MRI protocols in Neuroradiology [published online ahead of print, 2020 Jun 18]. J Neuroradiol. 2020;S0150-9861(20)30197-8. doi:10.1016/j.neurad.2020.05.008).

[4] A. Chazot, J.A. Barrat, M. Gaha, R. Jomaah, J. Ognard, D. Ben Salem, Brain MRIs make up the bulk of the gadolinium footprint in medical imaging. J Neuroradiol. 47 (2020), 259-265.

[5] K.A. Layne, P.I. Dargan PI, J.R.H. Archer, D.M. Wood, Gadolinium deposition and the potential for toxicological sequelae - A literature review of issues surrounding gadolinium-based contrast agents. Br J Clin Pharmacol. 84 (2018), 2522-2534.

[6] V. Gulani, F. Calamante, F.G. Shellock, E. Kanal, S.B. Reeder, Gadolinium deposition in the brain: summary of evidence and recommendations. Lancet Neurol, 16 (2017), 564-570.

[7] https://www.ema.europa.eu/en/documents/referral/gadolinium-article-31-referral-emas-final-opinion-confirms-restrictions-use-linear-gadolinium-agents_en.pdf

[8] M. Le Fur, P. Caravan, The biological fate of gadolinium-based MRI contrast agents: a call to action for bioinorganic chemists. Metallomics 11 (2019), 240-254.

[9] M. Veiga, J.S. de Gois, P.C. Nascimento, D.L.G. Borges, D. Bohrer, Presence of other rare earth metals in gadolinium-based contrast agents, Talanta (2020), DOI: 10.1016/j.talanta.2020.120940.

[10] G. Pagano, P.J. Thomas, A. Di Nunzio, M. Trifuoggi, Human exposures to rare earth elements: Present knowledge and research prospects. Environ Res. 171 (2019), 493-500.

[11] M. Adeel, J.Y. Lee, M. Zain *et al.*, Cryptic footprints of rare earth elements on natural resources and living organisms. Environ Int. 127 (2019),785-800.

[12] J.A. Barrat, F. Keller, J. Amossé, R.N. Taylor, R.W. Nesbitt, T. Hirata, Determination of rare earth elements in sixteen silicate reference samples by ICP-MS after Tm addition and ion exchange separation, Geostandards Newsletter 20 (1996), 1, 133-140.

[13] J.A. Barrat, B. Zanda, F. Moynier, C. Bollinger, C. Liorzou, G. Bayon, Geochemistry of CI chondrites: Major and trace elements, and Cu and Zn isotopes. Geochim. Cosmochim. Acta 83 (2012), 79-92.

[14] J.A. Barrat, N. Dauphas, P. Gillet, C. Bollinger, J. Etoubleau, A. Bischoff, A. Yamaguchi, Evidence from Tm anomalies for non-CI refractory lithophile element proportions in terrestrial planets and achondrites. Geochim. Cosmochim. Acta, 176 (2016), 1-17.

[15] J.A. Barrat, G. Bayon, X. Wang, S. Le Goff, M.L. Rouget, B. Gueguen, D. Ben Salem, A new chemical separation procedure for the determination of rare earth elements and yttrium abundances in carbonates by ICP-MS. Talanta 219 (2020), 121244.

[16] P. Dulski, Interferences of oxide, hydroxide and chloride analyte species in the determination of rare earth elements in geological samples by inductively coupled plasma-mass spectrometry, Fresenius Journal of Analytical Chemistry 350 (1994), 194-203.

[17] C.D. Coryell, J.W. Chase, J.W. Winchester, A procedure for geochemical interpretation of terrestrial rare earth abundance patterns. J. Geophys. Res. 68 (1963), 559–566.

[18] A. Masuda, Regularities in variation of relative abundances of Lanthanide elements and an attempt to analyse separation index patterns of some minerals. J. Earth Sci. Nagoya Univ. 10 (1962), 173–187.

[19] E. Di Gregorio, G. Ferrauto, C. Furlan, S. Lanzardo, R. Nuzzi, E. Gianolio, S. Aime, The issue of gadolinium retained in tissues: insights on the role of metal complex stability by

comparing metal uptake in murine tissues upon the concomitant administration of lanthanum- and gadolinium-diethylentriamminopentaacetate. Invest Radiol 53 (2018), 167-172.

[20] L.A. Henríquez-Hernández, D. Romero, A. González-Antuña, B. Gonzalez-Alzaga, M. Zumbado, L.D. Boada, A.F. Hernández, I. López-Flores, O.P. Luzardo, M. Lacasaña, Biomonitoring of 45 inorganic elements measured in plasma from Spanish subjects: a cross-sectional study in Andalusian population. Science of the Total Environment 706 (2020) 135750

Table 1. ICP-MS instrument operating conditions

RF power	1200 W
Sample uptake rate	100 µl / min
Coolant argon flow rates	16 l / min
Auxiliary argon flow rates	0.9 l / min
Nebuliser argon flow rates	1.031 l / min
Torch	Quartz
Nebuliser	PFA ST micro-flow
Spray chamber	Quartz cyclonic
Cones	Nickel
Low resolution mode (LRM)	^{7}Li, ^{9}Be, ^{89}Y, ^{90}Zr, ^{93}Nb, ^{121}Sb, ^{125}Te, ^{133}Cs, ^{135}Ba, ^{139}La, ^{140}Ce, ^{141}Pr, ^{143,146}Nd, ^{147,149}Sm, ^{151}Eu, ^{159}Tb, ^{163}Dy, ^{165}Ho, ^{167}Er, ^{169}Tm, ^{174}Yb, ^{175}Lu, ^{177,178}Hf, ^{181}Ta, ^{182,184,186}W, ^{205}Tl, ^{208}Pb, ^{209}Bi, ^{232}Th, ^{238}U
Medium resolution mode (MRM)	^{7}Li,^{31}P, ^{45}Sc, ^{47}Ti, ^{51}V, ^{52}Cr, ^{59}Co, ^{60}Ni, ^{63}Cu,^{66}Zn, ^{69}Ga, ^{85}Rb, ^{88}Sr, ^{90}Zr, ^{93}Nb, ^{111}Cd, ^{133}Cs, ^{181}Ta, ^{208}Pb
High resolution mode (HRM)	^{39}K, ^{45}Sc, ^{52}Cr, ^{139}La, ^{140}Ce, ^{141}Pr, ^{143,146}Nd, ^{147,149}Sm, ^{151}Eu, ^{152}Gd, ^{159}Tb, ^{163}Dy, ^{165}Ho, ^{167}Er, ^{169}Tm, ^{174}Yb, ^{175}Lu
Acquisition mode	Mass Accuracy
Number of scans	3*2
Ion lens settings	Acquisition to obtain maximum signal intensity
Wash time	100 s

Table 2. REE, Y, Ba and Pb abundances in GBCAs and in Allende chondrite USNM3529 (in ng/g). Gadolinium abundances in GBCAs were estimated based on concentrations and densities provided by pharmaceutical companies.

#	batch	exp.	Y	Ba	La	Ce	Pr	Nd	Sm	Eu	Gd	Tb	Dy	Ho	Er	Pb
			ng/g	ng/g	ng/g	ng/g	ng/g	ng/g	ng/g	ng/g	ng/g	ng/g	ng/g	ng/g	ng/g	ng/g
Dotarem®																
A	18GS783B	12/2021	1.5	102	2	11	0.4	0.4	0.9	21	6.69E+07	227	16	2	0.6	7
B	19GS706B	01/2022	4.4	91	3	21	0.7	0.7	0.8	18	6.69E+07	228	15	1	1.1	5
C	19GS723A	01/2022	5.5	65	2	11	0.6	0.6	0.9	20	6.69E+07	223	15	1	0.8	5
D	196S734A	05/2022	1.4	69	2	20	0.8	0.5	0.5	22	6.69E+07	221	13	1	0.5	6
E	19GS767B	07/2022	3.5	54	3	14	0.5	1.1	0.4	31	6.69E+07	222	12	3	0.5	10
Clariscan®																
A	14778806	09/2021	222	30	11	2	1.2	37	350	436	6.69E+07	282	22	2	0.1	15
B	14892151	11/2021	214	-	11	4	1.5	40	355	444	6.69E+07	349	22	2	0.5	18
C	14935977	12/2021	139	-	10	1	1.0	30	305	403	6.69E+07	330	20	2	0.3	18
D	14973656	01/2022	239	-	11	3	1.2	19	196	298	6.69E+07	332	25	3	0.4	26
E	14973656	01/2022	264	-	11	1	1.3	20	207	308	6.69E+07	274	24	3	0.2	14
Gadovist®																
A	KT04B67	07/2022	44	11	150	26	35	220	103	196	1.21E+08	426	93.3	12	6	1
B	KT04B69	08/2022	61	5	99	36	43	173	99	166	1.21E+08	421	119	25	9	0
C	KT04V02	09/2022	42	-	76	28	28	108	32	78	1.21E+08	495	91.9	17	6	1
D	KT056TK	11/2022	89	21	161	26	98	163	90	74	1.21E+08	618	205	49	55	7
E	KT056TK	11/2022	84	14	152	24	91	157	88	72	1.21E+08	600	201	47	54	1

Table 2 (continue). REE, Y, Ba and Pb abundances in GBCAs and in Allende chondrite USNM3529 (in ng/g). Gadolinium abundances in GBCAs were estimated based on concentrations and densities provided by companies.

#	lot	exp.	Y	Ba	La	Ce	Pr	Nd	Sm	Eu	Gd	Tb	Dy	Ho	Er	Pb
			ng/g	ng/g	ng/g	ng/g	ng/g	ng/g	ng/g	ng/g	ng/g	ng/g	ng/g	ng/g	ng/g	ng/g
ProHance®																
A	9C98026	02/2022	28	1	14	12	9	80	27	130	6.92E+07	337	43	4	3	1
B	9D99073	03/2022	8	1	2	16	3	1	1	8	6.92E+07	355	18	1	1	2
C	9E01301	04/2022	5	2	1	7	2	1	1	8	6.92E+07	325	16	1	1	1
D	9I05861	08/2022	30	1	15	12	10	103	25	194	6.92E+07	332	46	4	3	0.3
E	9L09263	11/2022	24	1	17	10	31	105	23	241	6.92E+07	329	31	2	1	0.3
MultiHance®																
A	SP7272M	09/2020	5	37	2	13	0.3	1	1	5	6.44E+07	255	13	1	0.6	4
B	SP8104D	04/2021	9	64	3	15	2	1	1	7	6.44E+07	287	15	3	0.8	5
C	Z19801D	12/2021	5	73	3	27	1	1	1	13	6.44E+07	277	14	1	0.9	3
Allende USNM3529																
n=5			2825	4460	506	1250	195	984	316	109	394	72.5	480	102	297	1177
RSD %			1.9	2.0	1.9	2.4	1.3	1.0	1.2	1.0	0.5	0.8	0.8	1.1	0.7	4.8
Barrat et al. [13]			2880	4530	516	1290	201	1020	329	114	417	76.2	508	107	310	1270

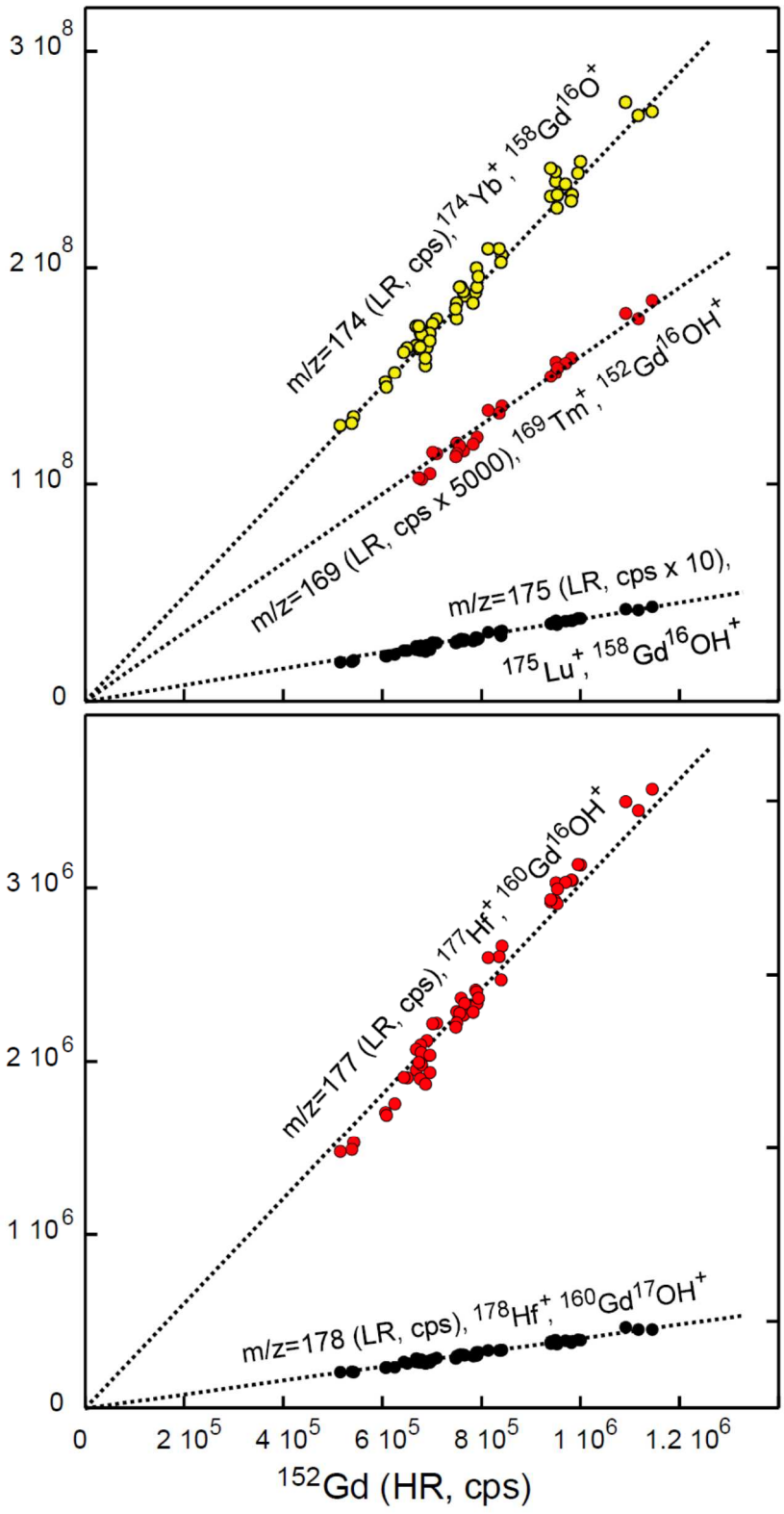

Fig. 1. Signals obtained on masses 169, 174, 175 (a), 177 and 178 (b) in low resolution compared to the signal obtained for ^{152}Gd in high resolution for various GBCA samples during an ICP-MS session.

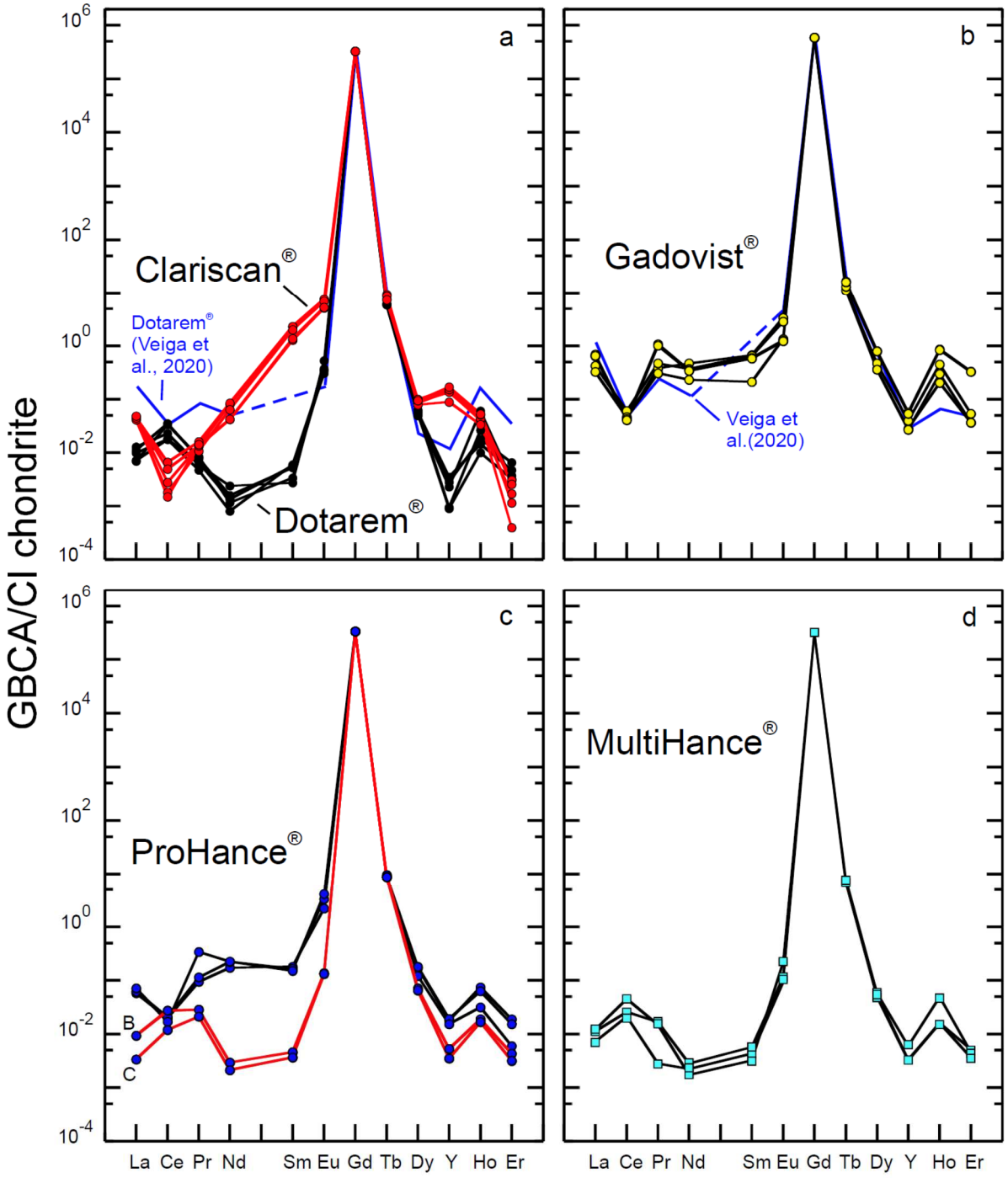

Figure 2. REE+Y patterns normalised to CI-chondrite [13] for GBCAs. The results obtained by Veiga et al. [9] are shown for comparison. Notice that Sm was not determined by these authors.

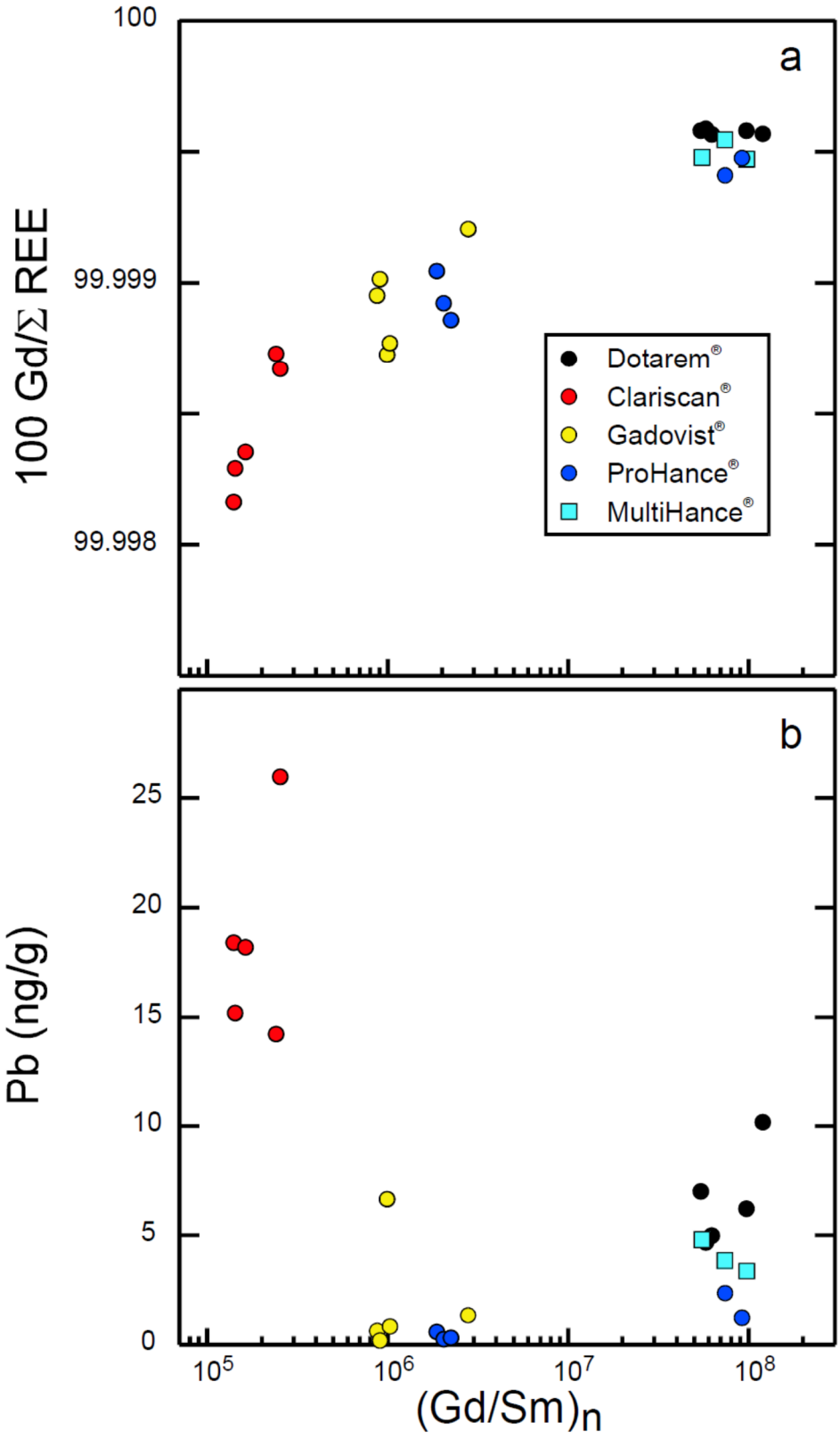

Figure 3. 100 Gd/ΣREE (a) and Pb (b) vs (Gd/Sm)n. ΣREE is the sum of the abundances (in ng/g) of the different REEs from La to Er.

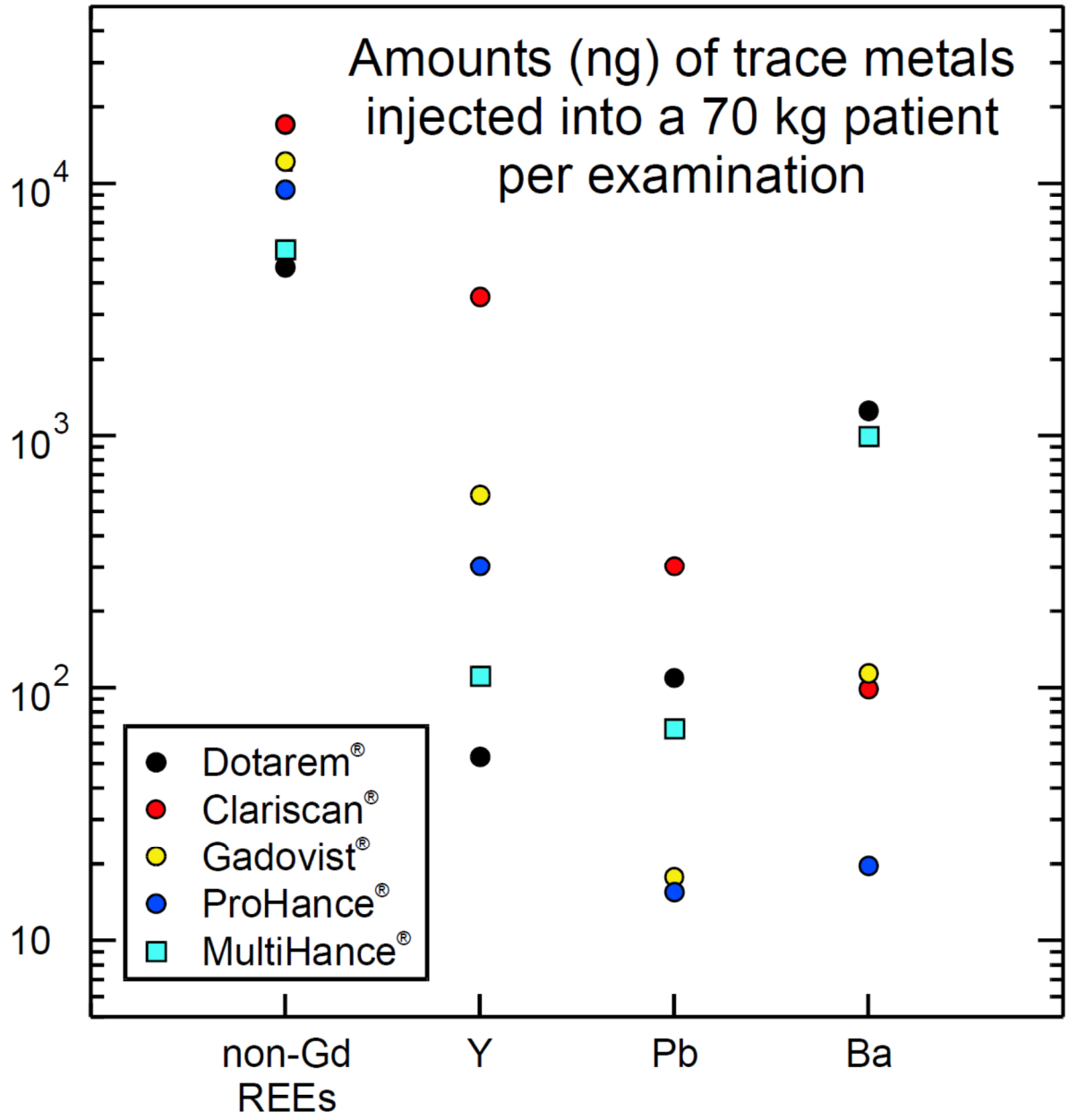

Figure 4. Amounts of trace metals injected into a 70 kg patient per examination. The averages of the concentrations given in Table 2 were used for the calculations, and converted in ng/ml using the densities of the GBCAs given by the pharmaceutical laboratories (Dotarem® and Clariscan®: 1.175, Gadovist®: 1.3; ProHance®: 1.137; MultiHance®: 1.22).

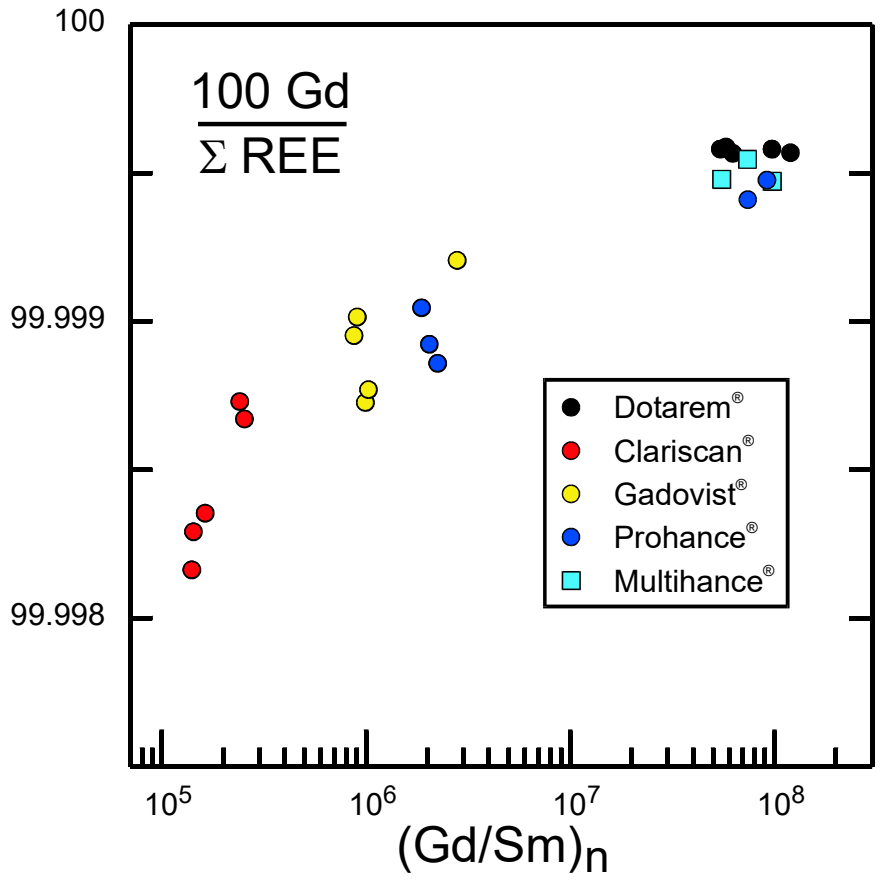
100
99.999
99.998
100 Gd
Σ REE
Dotarem®
Clariscan®
Gadovist®
Prohance®
Multihance®
10^5
10^6
10^7
10^8
(Gd/Sm)n